

EDITORS

GUOZHEN SHEN | ZHENG LOU | DI CHEN

FLEXIBLE SUPERCAPACITORS

MATERIALS AND APPLICATIONS

WILEY

Flexible Supercapacitors

Flexible Supercapacitors

Materials and Applications

Edited by

Guozhen Shen

*State Key Laboratory for Superlattices and Microstructures
Beijing, China*

Zheng Lou

*State Key Laboratory for Superlattices and Microstructures
Beijing, China*

Di Chen

*University of Science and Technology
Beijing, China*

WILEY

This edition first published 2022
© 2022 John Wiley & Sons, Inc

All rights reserved. No part of this publication may be reproduced, stored in a retrieval system, or transmitted, in any form or by any means, electronic, mechanical, photocopying, recording or otherwise, except as permitted by law. Advice on how to obtain permission to reuse material from this title is available at <http://www.wiley.com/go/permissions>.

The right of Guozhen Shen, Zheng Lou and Di Chen to be identified as the authors of the editorial material in this work has been asserted in accordance with law.

Registered Office

John Wiley & Sons, Inc., 111 River Street, Hoboken, NJ 07030, USA

Editorial Office

111 River Street, Hoboken, NJ 07030, USA

For details of our global editorial offices, customer services, and more information about Wiley products visit us at www.wiley.com.

Wiley also publishes its books in a variety of electronic formats and by print-on-demand. Some content that appears in standard print versions of this book may not be available in other formats.

Limit of Liability/Disclaimer of Warranty

In view of ongoing research, equipment modifications, changes in governmental regulations, and the constant flow of information relating to the use of experimental reagents, equipment, and devices, the reader is urged to review and evaluate the information provided in the package insert or instructions for each chemical, piece of equipment, reagent, or device for, among other things, any changes in the instructions or indication of usage and for added warnings and precautions. While the publisher and authors have used their best efforts in preparing this work, they make no representations or warranties with respect to the accuracy or completeness of the contents of this work and specifically disclaim all warranties, including without limitation any implied warranties of merchantability or fitness for a particular purpose. No warranty may be created or extended by sales representatives, written sales materials or promotional statements for this work. The fact that an organization, website, or product is referred to in this work as a citation and/or potential source of further information does not mean that the publisher and authors endorse the information or services the organization, website, or product may provide or recommendations it may make. This work is sold with the understanding that the publisher is not engaged in rendering professional services. The advice and strategies contained herein may not be suitable for your situation. You should consult with a specialist where appropriate. Further, readers should be aware that websites listed in this work may have changed or disappeared between when this work was written and when it is read. Neither the publisher nor authors shall be liable for any loss of profit or any other commercial damages, including but not limited to special, incidental, consequential, or other damages.

Library of Congress Cataloging-in-Publication Data

Names: Shen, Guozhen (Electrical engineer), editor. | Lou, Zheng, editor. | Chen, Di, editor.

Title: Flexible supercapacitors : materials and applications / edited by Guozhen Shen, State Key Laboratory for Superlattices and Microstructures, Beijing, China, Zheng Lou, State Key Laboratory for Superlattices and Microstructures, Beijing, China, Di Chen, University of Science and Technology, Beijing, China.

Description: First edition. | Hoboken, NJ : John Wiley & Sons, Inc., 2022. | Includes bibliographical references and index.

Identifiers: LCCN 2021052431 (print) | LCCN 2021052432 (ebook) | ISBN 9781119506164 (hardback) | ISBN 9781119506188 (obook) | ISBN 9781119506171 (epdf) | ISBN 9781119506157 (epub)

Subjects: LCSH: Supercapacitors. | Flexible electronics.

Classification: LCC TK7872.C65 F555 2022 (print) | LCC TK7872.C65 (ebook) | DDC 621.31/5--dc23/eng/20211207

LC record available at <https://lcn.loc.gov/2021052431>

LC ebook record available at <https://lcn.loc.gov/2021052432>

Cover Design: Wiley

Cover Image: © draganab/Getty Images

Set in 9.5/12.5pt STIXTwoText by Straive, Pondicherry, India

Contents

List of Contributors *xi*

Preface *xv*

1 Flexible Asymmetric Supercapacitors: Design, Progress, and Challenges *1*

Dun Lin, Xiyue Zhang and Xihong Lu

- 1.1 Introduction *1*
- 1.2 Configurations of AFSCs Device *3*
- 1.3 Progress of Flexible AFSCs *4*
 - 1.3.1 Sandwich-Type AFSCs *4*
 - 1.3.1.1 Carbon-Based Anodes *5*
 - 1.3.1.2 Transition Metal Oxide Anodes *6*
 - 1.3.1.3 Transition Metal Nitride Anodes *7*
 - 1.3.1.4 Conductive Polymer Anodes *9*
 - 1.3.2 Fiber-Type ASCs *9*
 - 1.3.2.1 Parallel-Type Fiber AFSCs *9*
 - 1.3.2.2 Wrap-Type Fiber AFSCs *10*
 - 1.3.2.3 Coaxial-Helix-Type Fiber AFSCs *12*
 - 1.3.2.4 Two-Ply-Yarn-Type AFSCs *13*
- 1.4 Summary *13*
- References *15*

2 Stretchable Supercapacitors *19*

La Li and Guozhen Shen

- 2.1 Overview of Stretchable Supercapacitors *19*
- 2.2 Fabrication of Stretchable Supercapacitor *20*
 - 2.2.1 Structures of Stretchable Fiber-Shaped SCs *20*
 - 2.2.1.1 Fabrication of Stretchable Parallel SCs *23*
 - 2.2.1.2 Fabrication of Stretchable Twisted SCs *25*
 - 2.2.1.3 Fabrication of Stretchable Coaxial SCs *27*
 - 2.2.2 Planar Stretchable SCs *29*
 - 2.2.2.1 Fabrication of the Stretchable Planar SCs with Sandwich Structure *29*
 - 2.2.2.2 Omnidirectionally Stretchable Planar SCs *29*
 - 2.2.2.3 Stretchable On-Chip Micro Supercapacitors (MSCs) *33*
 - 2.2.3 3D Stretchable SCs *36*
 - 2.2.3.1 Cellular Structure *36*

- 2.2.3.2 Editable SCs 38
- 2.3 Multifunctional Supercapacitor 40
- 2.3.1 Compressible SCs 40
- 2.3.2 Self-Healable SCs 42
- 2.3.3 Stretchable Integrated System 42
- 2.3.4 Perspective 47
- References 48

3 Fiber-shaped Supercapacitors 53

Mengmeng Hu, Qingjiang Liu, Yao Liu, Jiaqi Wang, Jie Liu, Panpan Wang, Hua Wang and Yan Huang

- 3.1 Introduction 53
- 3.2 Structure of FSSCs 54
- 3.3 Electrolyte 55
- 3.4 Electrode 58
- 3.4.1 Carbon-Based Materials 58
- 3.4.2 Conducting Polymers 59
- 3.4.3 Metal-Based Materials 61
- 3.4.4 Mxenes 62
- 3.4.5 Metal Organic Frameworks (MOFs) 62
- 3.4.6 Polyoxometalates (POMs) 63
- 3.4.7 Black Phosphorus (BP) 64
- 3.5 Electrode Design of FSSCs 64
- 3.5.1 Metal-Fiber Supported Electrode 64
- 3.5.2 Carbon Materials Based Fiber Supported Electrode 67
- 3.5.2.1 Carbon Fiber 69
- 3.5.2.2 CNT Fiber 69
- 3.5.2.3 Graphene Fiber 72
- 3.5.3 Cotton Fiber Supported Electrode 73
- 3.6 Functionalized FSSCs 74
- 3.6.1 Self-Healable FSSCs 74
- 3.6.2 Stretchable FSSCs 76
- 3.6.3 Electrochromic FSSCs 77
- 3.6.4 Shape-Memory FSSCs 80
- 3.6.5 Photodetectable FSSCs 80
- 3.7 Conclusion 81
- References 83

4 Flexible Fiber-shaped Supercapacitors: Fabrication, Design and Applications 91

Muhammad S. Javed, Peng Sun, Muhammad Imran and Wenjie Mai

- 4.1 Introduction to Fiber-Shaped Supercapacitors 91
- 4.2 Emerging Techniques for the Fabrication of Fiber-Shaped Electrodes 93
- 4.2.1 Wet Spinning Method 93
- 4.2.2 Spray/Cast-Coating Method 95
- 4.2.3 Hydrothermal Method 95
- 4.3 Structures and Design/Configuration of Fiber-Shaped Electrodes 95
- 4.3.1 Parallel-Fiber Electrodes 95
- 4.3.2 Twisted-Fiber Electrodes 96

- 4.3.3 Coaxial-Fiber Electrodes 100
- 4.3.4 Rolled-Fiber Electrodes 102
- 4.4 Materials for Fiber-shaped Supercapacitors 104
 - 4.4.1 Carbon-Based Materials for FFSC 104
 - 4.4.2 Metal Oxides and Their Composites-Based Materials for FFSC 107
- 4.5 Electrolytes for Fiber-Shaped Supercapacitors 109
- 4.6 Performance Evaluation Metrics for Fiber-Shaped Supercapacitors 110
- 4.7 Applications 111
- 4.8 Conclusion and Future Prospectus 113
- Acknowledgments 114
- References 114

5 Flexible Supercapacitors Based on Ternary Metal Oxide (Sulfide, Selenide) Nanostructures 121

Qiuhan Wang, Daohong Zhang and Guozhen Shen

- 5.1 Introduction 121
 - 5.1.1 Background of Electrochemical Capacitors 121
 - 5.1.2 Performance Evaluation of SCs 122
- 5.2 Ternary Metal Oxide 123
 - 5.2.1 1D Ternary Metal Oxide Nanostructured Electrodes 123
 - 5.2.2 2D Ternary Metal Oxide Nanostructured Electrodes 125
 - 5.2.3 3D Ternary Oxide Electrodes 127
 - 5.2.4 Core-Shell Ternary Metal Oxide Composite Electrode 128
 - 5.2.4.1 Core-Shell Nanoarrays 128
- 5.3 Metal Sulfide Electrodes 131
 - 5.3.1 1D Metal Sulfide Electrodes 132
 - 5.3.2 2D Metal Sulfide Electrodes 133
 - 5.3.3 3D Metal Sulfide Electrodes 135
 - 5.3.4 Metal Sulfide Composite Electrodes 135
- 5.4 Metal Selenide Electrodes 143
 - 5.4.1 1D Metal Selenide 144
 - 5.4.2 2D Metal Selenide Electrodes 145
 - 5.4.3 3D Metal Selenide Electrodes 146
- 5.5 Fiber-Shaped SCs 147
- 5.6 Summary and Perspectives 152
- Declaration of Competing Interest 154
- Acknowledgments 154
- References 154

6 Transition Metal Oxide Based Electrode Materials for Supercapacitors 157

Xiang Wu

- 6.1 Introduction 157
- 6.2 Co_3O_4 Electrode Materials 158
- 6.3 NiO Electrode Materials 163
- 6.4 Fe_2O_3 Electrode Materials 164
- 6.5 MnO_2 Electrode Materials 169
- 6.6 V_2O_5 Electrode Materials 174
- References 176

7	Three-Dimensional Nanoarrays for Flexible Supercapacitors	179
	<i>Jing Xu</i>	
	List of Abbreviations	179
7.1	Introduction	180
7.2	Fabrication of 3D Nanoarrays	181
7.2.1	Selection of Substrates	181
7.2.1.1	Metal Foils	181
7.2.1.2	Polymeric Films	181
7.2.1.3	Textile-Like Materials	181
7.2.2	Synthesis Methods of Flexible 3D Nanoarrays	182
7.2.2.1	Flexible 3D Nanoarray Electrodes Fabricated by Hydrothermal Methods	182
7.2.2.2	Flexible 3D Nanoarray Electrodes Fabricated by CVD/Sputtering Methods	183
7.2.2.3	Flexible 3D Nanoarray Electrodes Fabricated by Electrochemical Deposition Methods	183
7.3	Typical Structural Engineering of 3D Nanoarrays for Flexible Supercapacitors	186
7.3.1	Basic 3D Nanoarrays for Flexible Supercapacitors	188
7.3.1.1	Flexible Electrical Double-Layer Capacitors	188
7.3.1.2	Flexible Pseudocapacitors	189
7.3.2	Hybrid 3D Nanoarrays for Flexible Supercapacitors	194
7.3.2.1	Doping of Heteroatoms and Anchoring of Functional Groups	194
7.3.2.2	Pre-Intercalation of Heteroatoms	194
7.3.2.3	Coaxial Branched and Core-Shell 3D Hybrid Nanostructures	195
7.4	Evaluation of Flexible Supercapacitors	198
7.4.1	Bending Deformation	198
7.4.2	Stretching Deformation	198
7.4.3	Twisting Deformation	200
7.5	Conclusion	200
	Acknowledgments	201
	References	201
8	Metal Oxides Nanoarray Electrodes for Flexible Supercapacitors	205
	<i>Ting Meng and Cao Guan</i>	
8.1	Introduction	205
8.2	Synthesis Techniques of Metal Oxide Nanoarrays	207
8.2.1	Solution-based Route	207
8.2.2	Electrodeposition Growth	210
8.2.3	Chemical Vapor Deposition	210
8.3	The Flexible Support Substrate for Loading Nanoarrays	213
8.3.1	3D Porous Graphene Foam	213
8.3.2	Carbon Cloth Current Collectors	213
8.3.3	Metal Conductive Substrates	215
8.4	The Geometry of Nanostructured Arrays	220
8.4.1	The 1D Nanostructured Arrays	221
8.4.2	The 2D Nanostructured Arrays	224
8.4.3	The Integration of 1D@2D Nanoarrays	226
8.5	Conclusions and Prospects	228
	References	230

9	Printed Flexible Supercapacitors	235
	<i>Yizhou Zhang and Wen-Yong Lai</i>	
	List of Abbreviations	235
9.1	Overview of Printed Flexible Supercapacitor	236
9.2	Devices Structure of Printed SCs	238
9.3	Printable Materials for SCs	239
9.3.1	Electrodes Materials	239
9.3.1.1	Carbon-Based Materials	239
9.3.1.2	Metal Oxides	240
9.3.1.3	2D Transition Metal Carbides, Nitrides, and Carbonitrides (MXenes)	240
9.3.1.4	Metal-Organic Frameworks (MOFs)	241
9.3.2	Electrolytes	241
9.3.2.1	Aqueous Gel Polymer Electrolytes	242
9.3.2.2	Organic Gel Polymer Electrolytes	242
9.3.2.3	Ionic Liquid-Based Gel Polymer Electrolytes	242
9.3.2.4	Redox-Active Gel Electrolytes	243
9.3.3	Flexible Substrates	243
9.3.3.1	Metal Substrates	243
9.3.3.2	Synthetic Polymer-Based Substrates	243
9.4	Fabrication of Flexible SCs Using Various Printing Methods	244
9.4.1	Inkjet Printing	244
9.4.2	Screen Printing	247
9.4.3	Transfer Printing	249
9.4.4	3D Printing	251
9.5	Printed Integrated System	254
9.6	Perspective	255
	Acknowledgments	257
	References	258
10	Printing Flexible On-chip Micro-Supercapacitors	261
	<i>Guozhen Shen</i>	
10.1	Introduction	261
10.2	Printable Materials for On-chip MSCs	262
10.2.1	Printable Electrode Materials	262
10.2.2	Printable Current Collector	267
10.2.3	Printable Electrolyte	269
10.3	Printing Techniques	270
10.3.1	Inkjet Printing	270
10.3.2	Spray Printing	273
10.3.3	Screen Printing	274
10.3.4	3D Printing	275
10.4	Summary	277
	References	277
11	Recent Advances of Flexible Micro-Supercapacitors	283
	<i>Songshan Bi, Hongmei Cao, Rui Wang and Zhiqiang Niu</i>	
11.1	Introduction	283
11.2	General Features of Flexible MSCs	284

11.3	Active Materials of Flexible MSCs	286
11.3.1	Graphene-based Materials	287
11.3.2	CNT-based Materials	290
11.3.3	Other Carbon-based Materials	293
11.3.4	Transition Metal Oxides and Hydroxides	293
11.3.5	MXenes	296
11.3.6	Conductive Polymer	297
11.4	Integration of Flexible MSCs	298
11.4.1	Flexible Self-charging MSCs	298
11.4.2	Flexible Self-powering MSCs	298
11.5	Flexible Smart MSCs	302
11.5.1	Flexible Self-healing MSCs	302
11.5.2	Flexible Electrochromic MSCs	302
11.5.3	Flexible Photodetectable MSCs	304
11.5.4	Flexible Thermoreversible Self-protecting MSCs	304
11.6	Summary and Prospects	305
	References	307

Index	313
--------------	-----

List of Contributors

Songshan Bi

Key Laboratory of Advanced Energy Materials
Chemistry (Ministry of Education)
College of Chemistry, Nankai University
Tianjin, 300071, P. R. China

Hongmei Cao

Key Laboratory of Advanced Energy Materials
Chemistry (Ministry of Education)
College of Chemistry, Nankai University
Tianjin, 300071, P. R. China

Cao Guan

Frontiers Science Center for Flexible
Electronics, Institute of Flexible Electronics
Northwestern Polytechnical University
Xi'an, 710072, P.R. China

Mengmeng Hu

State Key Laboratory of Advanced Welding
and Joining
Harbin Institute of Technology (Shenzhen)
Shenzhen 518055, Guangzhou, China; and
Flexible Printed Electronics Technology Centre
Harbin Institute of Technology (Shenzhen)
Shenzhen 518055, Guangzhou, China

Yan Huang

State Key Laboratory of Advanced Welding
and Joining
Harbin Institute of Technology (Shenzhen)
Shenzhen 518055, Guangzhou, China; and
Flexible Printed Electronics Technology Centre
Harbin Institute of Technology (Shenzhen)
Shenzhen 518055, Guangzhou, China; and
School of Materials Science and Engineering
Harbin Institute of Technology (Shenzhen)
Shenzhen 518055, Guangzhou, China

Muhammad Imran

Department of Chemistry, Faculty of Science
King Khalid University
Abha 61413, Saudi Arabia

Muhammad S. Javed

School of Physical Science and Technology
Lanzhou University
Lanzhou 730000, PR China; and
Siyuan Laboratory, Guangdong Provincial
Engineering Technology Research Center
of Vacuum Coating Technologies and
New Energy Materials, Department of Physics
Jinan University
Guangzhou 510632, PR China

Wen-Yong Lai

State Key Laboratory of Organic Electronics
and Information Displays (SKLOEI), Institute
of Advanced Materials (IAM)
Nanjing University of Posts &
Telecommunications
9 Wenyuan Road, Nanjing 210023, Jiangsu,
China; and
Frontiers Science Center for Flexible
Electronics (FSCFE), MIIT Key Laboratory of
Flexible Electronics (KLoFE)
Northwestern Polytechnical University
127 West Youyi Road, Xi'an 710072,
Shaanxi, China

La Li

State Key Laboratory for Superlattices and
Microstructures
Institute of Semiconductors, Chinese Academy
of Science
Beijing 100083, China

Dun Lin

MOE of the Key Laboratory of Bioinorganic and Synthetic Chemistry, The Key Lab of Low-Carbon Chem and Energy Conservation of Guangdong Province, School of Chemistry Sun Yat-Sen University, Guangzhou Guangzhou, 510275, People's Republic of China

Jie Liu

State Key Laboratory of Advanced Welding and Joining Harbin Institute of Technology (Shenzhen) Shenzhen, 518055, Guangzhou, China; and Flexible Printed Electronics Technology Centre Harbin Institute of Technology (Shenzhen) Shenzhen, 518055, Guangzhou, China

Qingjiang Liu

State Key Laboratory of Advanced Welding and Joining Harbin Institute of Technology (Shenzhen) Shenzhen, 518055, Guangzhou, China; and Flexible Printed Electronics Technology Centre Harbin Institute of Technology (Shenzhen) Shenzhen, 518055, Guangzhou, China

Yao Liu

State Key Laboratory of Advanced Welding and Joining Harbin Institute of Technology (Shenzhen) Shenzhen, 518055, Guangzhou, China; and Flexible Printed Electronics Technology Centre Harbin Institute of Technology (Shenzhen) Shenzhen, 518055, Guangzhou, China

Xihong Lu

MOE of the Key Laboratory of Bioinorganic and Synthetic Chemistry, The Key Lab of Low-Carbon Chem and Energy Conservation of Guangdong Province, School of Chemistry Sun Yat-Sen University, Guangzhou Guangdong, 510275, People's Republic of China

Wenjie Mai

Siyuan Laboratory, Guangdong Provincial Engineering Technology Research Center of Vacuum Coating Technologies and New Energy Materials, Department of Physics Jinan University Guangzhou, 510632, PR China

Ting Meng

Frontiers Science Center for Flexible Electronics, Institute of Flexible Electronics Northwestern Polytechnical University Xi'an, 710072, P. R. China

Zhiqiang Niu

Key Laboratory of Advanced Energy Materials Chemistry (Ministry of Education), College of Chemistry Nankai University Tianjin, 300071, P. R. China

Guozhen Shen

State Key Laboratory for Superlattices and Microstructures Institute of Semiconductors, Chinese Academy of Science Beijing, 100083, China

Peng Sun

Siyuan Laboratory, Guangdong Provincial Engineering Technology Research Center of Vacuum Coating Technologies and New Energy Materials, Department of Physics Jinan University Guangzhou, 510632, PR China

Hua Wang

State Key Laboratory of Advanced Welding and Joining Harbin Institute of Technology (Shenzhen) Shenzhen, 518055, Guangzhou, China; and Flexible Printed Electronics Technology Centre Harbin Institute of Technology (Shenzhen) Shenzhen, 518055, Guangzhou, China

Jiaqi Wang

State Key Laboratory of Advanced Welding and Joining
Harbin Institute of Technology (Shenzhen)
Shenzhen, 518055, Guangzhou, China; and
Flexible Printed Electronics
Technology Centre
Harbin Institute of Technology (Shenzhen)
Shenzhen, 518055, Guangzhou, China

Panpan Wang

State Key Laboratory of Advanced Welding and Joining
Harbin Institute of Technology (Shenzhen)
Shenzhen, 518055, Guangzhou, China; and
Flexible Printed Electronics
Technology Centre
Harbin Institute of Technology (Shenzhen)
Shenzhen, 518055, Guangzhou, China

Qiufan Wang

Key laboratory of Catalysis and Energy Materials Chemistry of Ministry of Education & Hubei Key Laboratory of Catalysis and Materials Science, Hubei R&D Center of Hyperbranched Polymers Synthesis and Applications
South-Central University for Nationalities
182 Minzu Road, Wuhan, 430074, China

Rui Wang

Key Laboratory of Advanced Energy Materials Chemistry (Ministry of Education)
College of Chemistry, Nankai University
Tianjin, 300071, P. R. China

Xiang Wu

School of Materials Science and Engineering
Shenyang University of Technology
China

Jing Xu

School of Materials Science and Engineering
Nanjing University of Science and Technology
Xuanwu District, Nanjing 210094, China; and
Herbert Gleiter Institute of Nanoscience
Nanjing University of Science and Technology
Xuanwu District, Nanjing 210094, China

Daohong Zhang

Key laboratory of Catalysis and Energy Materials Chemistry of Ministry of Education & Hubei Key Laboratory of Catalysis and Materials Science, Hubei R&D Center of Hyperbranched Polymers Synthesis and Applications
South-Central University for Nationalities
182 Minzu Road, Wuhan 430074, China

Xiyue Zhang

MOE of the Key Laboratory of Bioinorganic and Synthetic Chemistry, The Key Lab of Low-Carbon Chem and Energy Conservation of Guangdong Province, School of Chemistry Sun Yat-Sen University
Guangzhou, Guangdong, 510275, People's Republic of China

Yizhou Zhang

State Key Laboratory of Organic Electronics and Information Displays (SKLOEI), Institute of Advanced Materials (IAM)
Nanjing University of Posts & Telecommunications
9 Wenyuan Road, Nanjing, 210023, Jiangsu, China; and
Institute of Advanced Materials and Flexible Electronics (IAMFE), School of Chemistry and Materials Science
Nanjing University of Information Science & Technology
219 Ningliu Road, 210044, Nanjing, Jiangsu, China

Preface

As an emerging and exciting research field, flexible electronics have attracted tremendous interests from both the academic and industrial communities. Till now, many kinds of flexible electronic devices and systems have been developed, such as flexible displays, electronic skins, health monitoring bioelectronics, chemical and biosensors, wearable smart textile, and intelligent soft robots, etc. This area develops very fast and some flexible products are already commercially available. For example, flexible organic light-emitting diode displays have been widely used in smart phones, smart watches, and tablet personal computers.

The booming development of flexible electronics has driven the demand for compatible flexible energy storage devices, ideally to make the whole electronic system flexible. Although conventional energy storage devices, such as lithium-ion batteries, lead acid batteries, supercapacitors, have been widely used in our modern society and affected our daily life, their rigid shape, heavy weight, and thickness make them not suitable for flexible electronics. Among different energy storage devices, supercapacitors have the advantages of simple device structure, high power density, short charge and discharge time, long cycle life and wide operating temperature range. When making supercapacitor flexible, it will also possess the required features of excellent flexibility, portability, stretchability, miniaturized size, ultrathin thickness for flexible electronic devices. During the past several years, researches on flexible supercapacitors are very active and this field expanded very fast. Thus, it is considered timely to provide a survey of a number of important developments in this field.

This book provides an up-to-date survey of the state of flexible supercapacitors. It contains a selection of 11 chapters contributed by a number of research teams. All the contributors are active researchers in the field of flexible supercapacitors. The most important topics related to flexible supercapacitors are included in this book, ranging from the selection and design of different active electrode materials, the design of different device structures, suitable fabrication techniques, and different functions. I hope this book will be a source of inspiration for graduate students, researchers, and industrial engineers, and will stimulate new developments in this challenging but exciting field.



Guozhen Shen, Professor
Beijing, China

1

Flexible Asymmetric Supercapacitors

Design, Progress, and Challenges

Dun Lin, Xiyue Zhang and Xihong Lu

MOE of the Key Laboratory of Bioinorganic and Synthetic Chemistry, The Key Lab of Low-Carbon Chem and Energy Conservation of Guangdong Province, School of Chemistry, Sun Yat-Sen University, Guangzhou, Guangdong, 510275, People's Republic of China

1.1 Introduction

Recently, flexible electronic products, such as flexible microphones [1], elastic circuits [2–4], pressure and strain sensors [5–7], artificial skin sensors [8–10], intelligent garments [11], and wearable health monitoring devices have boomed as a new and important field of modern electronics (Figure 1.1). Therefore, the development of suitable energy storage devices, which can serve as an excellent power supply while sustaining high mechanical flexibility, are becoming increasingly necessary to power these electronics [13–21]. Supercapacitors (SCs), also known as electrochemical capacitors or ultracapacitors, have emerged as the bridge between batteries and traditional capacitors due to their promising merits of high power density (about 10 kW kg^{-1}), good reversibility, excellent cyclic stability (over 10^6 cycles), and safety [22, 23]. Meanwhile, accompanied with the advanced development of lightweight, foldable, and stretchable materials, substantial effort has been invested in the fabrication of flexible supercapacitors (FSCs) [24–28].

In order to satisfy the further demand for practical usage, the configuration of the two electrodes as well as the geometry of the devices are of vital importance and worth careful considerations [29]. The major obstacle of early designed FSCs is their relatively low energy density (E) to mismatch basic requirements of future applications. Thus, tremendous efforts have been denoted to optimize the overall performance of FSCs according to the Eq. (1.1), without sacrificing their power density and service life.

$$E = \frac{1}{2} CV^2 \quad (1.1)$$

In general, either enhanced capacitance (C) or enlarged operating voltage (V) of the device should make sense. Of which, the C of a FSC device can be equivalent to the negative electrode capacitance (C_n) and positive electrode capacitance (C_p) connected in series (Figure 1.2a), which can be calculated using Eq. (1.2)

$$\frac{1}{C} = \frac{1}{C_n} + \frac{1}{C_p} \quad (1.2)$$

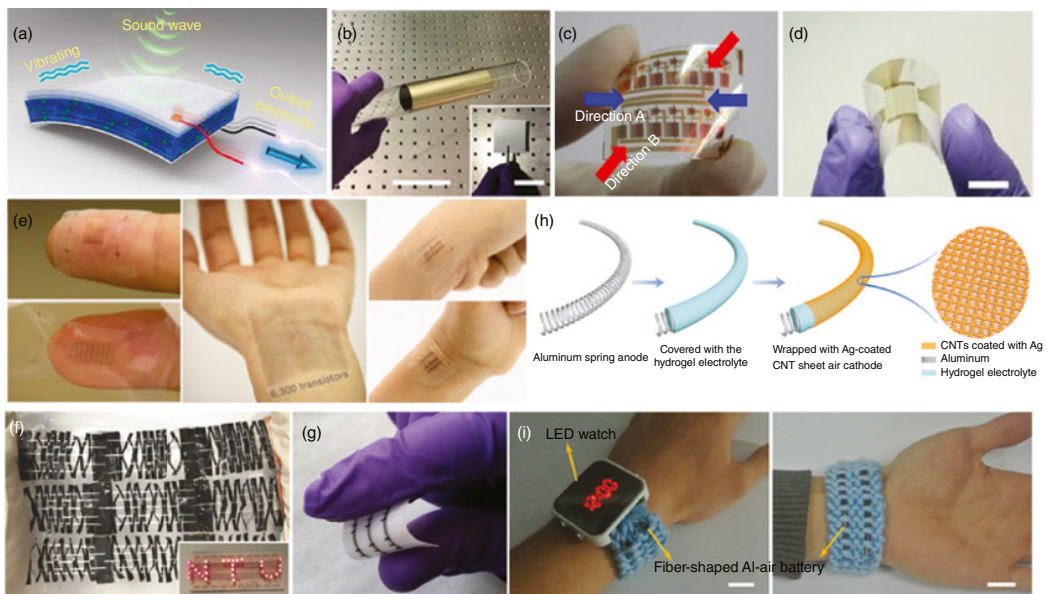


Figure 1.1 (a, b) Scheme and optical image of a flexible acoustic device. *Source:* Reproduced with permission from Ref. [121], © 2017, Springer Nature. Optical image of (c) a flexible circuit *Source:* Reproduced with permission from Ref. [2], © 2018, NPG, (d) multiplexed fingerprint sensor. Scale bar, 1 cm. *Source:* Reproduced with permission from Ref. [5], © 2018, NPG and (e) artificial skin electronics *Source:* Reproduced with permission from Ref. [8], © 2018, NPG. (f) 3×3 honeycomb-like supercapacitor array powering LED panel. *Source:* Reproduced with permission from Ref. [13], © 2017, Wiley. (g) Image of an array of field-effect heterojunctions on textile. *Source:* Reproduced with permission from Ref. [14], © 2017, NPG. (h, i) Fabrication and optical image of the fiber-shaped Al-air battery. *Source:* Reproduced with permission from Ref. [15], © 2016, Wiley.

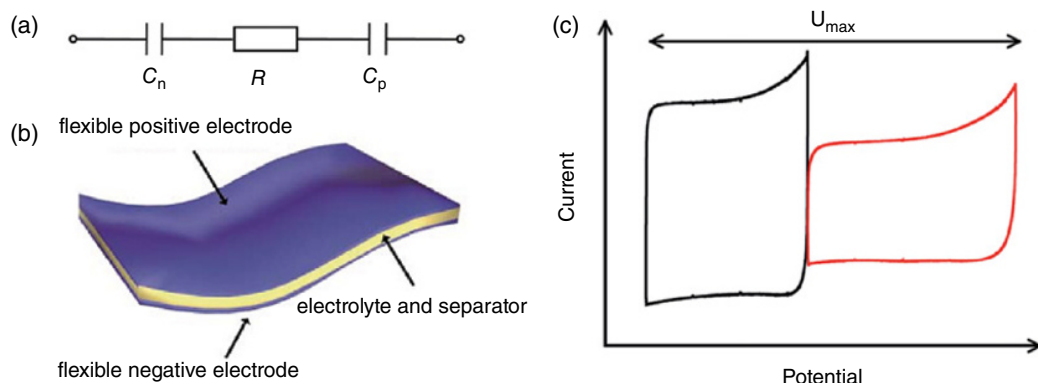


Figure 1.2 (a) The equivalent circuit of an AFSC. (b) Schematic illustration of the typical configuration of AFSCs and (c) Cyclic voltammograms (CV) curves as schematic illustrations of typical AFSCs. Source: Reproduced with permission [30]. © 2016, Royal Society of Chemistry.

The maximum C value of the FSCs can be reached when C_n is equal to C_p . Thus, early investigations focused on the symmetric flexible supercapacitors (SFSCs) with cathodes and anodes being identical for achieving higher device capacitance [31–34]. However, due to their limited potential voltage ($<1\text{ V}$ in aqueous electrolyte), the energy density of SFSCs is still unsatisfactory. Notably, the V of a FSC device related to the capacitive potential range of electrodes. Thus, asymmetric flexible supercapacitors (AFSCs), also called hybrid SCs or battery-capacitor SCs, are designed with different electrodes configured together (Figure 1.2b) [24–28]. By making use of the distinct capacitive potential range, AFSCs have been widely proven to effectively achieve high operating voltages (even $>2\text{ V}$ in aqueous electrolyte) as well as optimized capacitance after balancing the charge between the specific positive and negative electrodes (Figure 1.2c) [30, 35]. In addition, they have several important advantages including small size, low weight, ease of handling, excellent reliability, and a wider range of operating temperatures. Therefore, AFSCs have become one of the most promising energy storage devices for flexible and wearable electronics.

In this context, to achieve high electrochemical performance while maintaining good mechanical stability, FSCs with asymmetric structure could realize further gains, and thus arouse global efforts in relative research. This chapter enumerates some typical newly developed AFSCs in terms of structure design of electrode materials and device's configuration engineering. We first focus on the guidelines on the material design and charge balance of a typical AFSC device. Furthermore, different types of various newly developed AFSCs, including sandwich-type, fiber-type, and the other type of AFSCs devices, are illustrated based on various electrode materials. Finally, the future developing trends and challenges are discussed to provide certain reference to readers on how to contrive this device.

1.2 Configurations of AFSCs Device

Specifically, AFSCs device can be fabricated by constructing two flexible dissimilar electrodes (a Faradaic positive electrode and a capacitor-type negative electrode), a separator and, in most cases, quasi-solid-state electrolyte in a soft package. Among various types of quasi-solid-state

electrolytes, gel polymer electrolytes have been extensively used in FSCs due to its relatively high ionic conductivity [36–40]. Soft and bendable plastics including polyethylene terephthalate (PET) [41–44], polydimethylsiloxane (PDMS) [45], and ethylene/vinyl acetate copolymer (EVA) film [46] are typically used as packaging materials for FSC devices.

Considering that the fundamental limit of energy storage capability is largely determined by the electrode material, either the material choice or structure design of electrode materials are of vital importance. Apart from directly fabricated freestanding films like carbon nanotube (CNT) films [47, 48] and graphene films [49, 50], previous reports for FSCs indicate that the flexible electrodes can also rely on a flexible substrate such as thin metal foils [51, 52], polymer substrates [53], textiles [54], and papers [55], to provide flexibility. The main differences between the AFSCs and SFSCs are that the AFSCs require that the positive and negative electrodes are not the same, but they need to be matched well. Electrode materials that are dominated by Faradaic reactions such as metal oxides (RuO_2 [56, 57], MnO_2 [58–64], CoO [60, 65–67], NiO [68–70], V_2O_5 [71, 72], etc.), metal sulfides (NiCo_2S_4 [73–75], MoS_2 [76], CoS_2 [77, 78], NiS [58, 63, 79, 80], etc.) and conductive polymers (polyaniline (PANI) [32, 81], polypyrrole (PPy) [82, 83], poly (3,4-ethylenedioxythiophene) (PEDOT) [84, 85] etc.) are normally applied as positive electrodes in AFSCs due to their high specific capacitance and relatively higher potential window. Notably, carbon-based materials (activated carbon [60, 66, 67], graphene [59, 86], CNTs [87], carbon fibers [88–90] etc.), metal nitrides (TiN [20], VN [91], MoN [92], etc.), and some metal oxides (FeOx [93], MoOx [94] etc.) are usually employed as negative electrodes because of their fast charging/discharging rate and suitable working window at negative potential.

However, before they are assembled in an AFSC, the matching problems of the two electrodes with different theoretical capacitance need to be solved [91]. As for an AFSC, the charge balance will follow the relationship $q_+ = q_-$. The charge stored by each electrode depends on the specific capacitance (C), the potential range for the charge/discharge process (E) and the mass of the active electrode material (m), following the Eq. (1.3):

$$q = C \times E \times m \quad (1.3)$$

In order to get $q_+ = q_-$ at the typical current density, the mass balancing will follow the Eq. (1.4):

$$\frac{m_+}{m_-} = \frac{C_- \times E_-}{C_+ \times E_+} \quad (1.4)$$

In this way, the suitable mass ratio between the positive electrode (m_+) and negative electrode (m_-) is defined, which is much closed to the mass loading of the active materials of positive and negative electrode in typical AFSCs.

1.3 Progress of Flexible AFSCs

1.3.1 Sandwich-Type AFSCs

To date, the most widely applied configuration of AFSCs is sandwich-type AFSCs, which stacks two flexible flat electrodes face-to-face with an ionic conductive separator and liquid/gel electrolyte in the middle of the two electrodes to isolate direct contact. AFSCs with such shape holds great potential in future applications in flexible planar electronic devices, such as flexible display, wristbands, membrane-type sensors, etc. [24]

1.3.1.1 Carbon-Based Anodes

The most reliable anode materials for sandwich-type AFSCs are carbon-based materials with significant excellence in conductivity and mechanical stability, such as graphene, CNTs, carbon fibers, etc. [24, 25, 27, 56, 95–97] For example, Zhai et al. [98] successfully synthesized hydrogenated MnO_2 nanorods (H-MnO_2) on carbon cloth (CC) via electrodeposition followed by annealing in hydrogen atmosphere (Figure 1.3a), and loaded reduced graphene oxide (RGO) on CC using vacuum process. The obtained H-MnO_2 cathode and RGO anode were assembled as flexible solid-state AFSC with LiCl/PVA gel electrolyte and a separator sandwiched in between. The as-fabricated sandwich-type AFSC (denoted as $\text{H-MnO}_2/\text{RGO}$) exhibited a reliable operating voltage window as wide as 1.8 V and extraordinary mechanical tolerance to bending (Figure 1.3b). Owing to the significantly wide potential window, the device achieved a high energy density of 0.25 mWh cm^{-3} at power density of 1.01 W cm^{-3} , which has surpassed many SFSCs and some AFSCs previously reported. To verify the feasibility of the AFSCs device as energy storage device for wearable electronics, two $\text{H-MnO}_2/\text{RGO}$ devices were tailored on a laboratory coat in series and able to power an electronic watch (Figure 1.3c). Recently, Yu and his co-workers [25] reported a sandwich-type AFSC with CNT-textile anode and $\text{MnO}_2/\text{graphene-textile}$ cathode, which achieved an operating potential window of 1.5 V and a maximum energy density of 12.5 Wh kg^{-1} . Choi et al. [56] developed a solid-state AFSC based on an ionic liquid functionalized chemically modified graphene (IL-CMG) film as anode and a hydrous $\text{RuO}_2\text{-ILCMG}$ composite film as cathode, which reached a high output voltage of 1.8 V and thus delivered a maximum energy density of 19.7 Wh kg^{-1} and

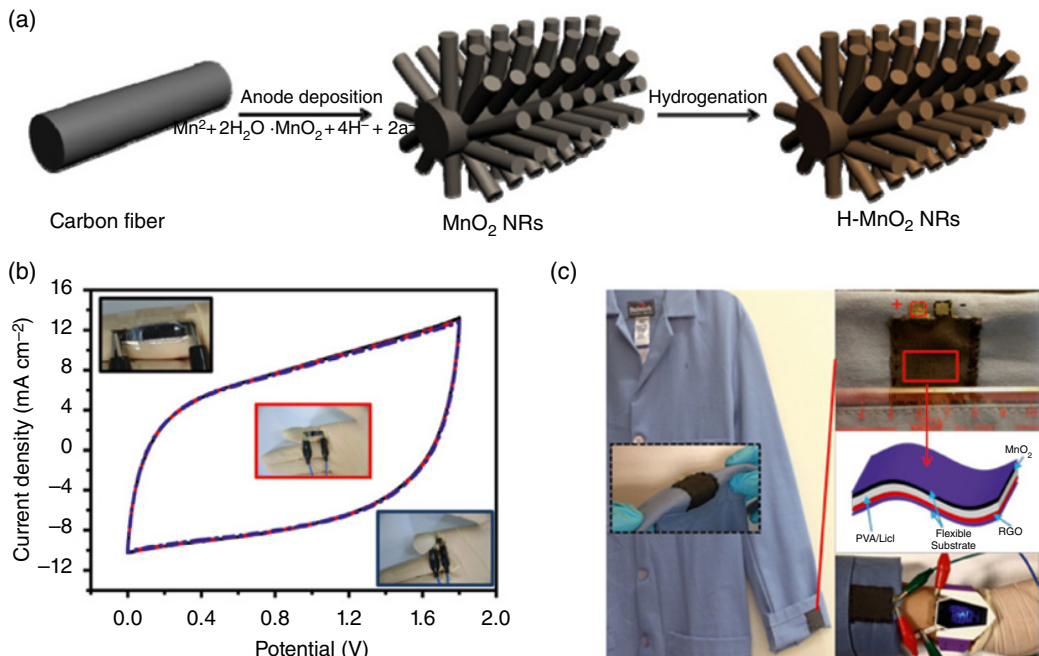


Figure 1.3 (a) Schematic diagram illustrates the growth process for preparing H-MnO_2 NRs on carbon cloth substrate. (b) CV curves obtained at different bent conditions at 200 mVs^{-1} . Insets are the photos of ACS device on finger. (c) Schematic diagram and photo images of wearable ACS in real applications (sewing on the clothes model and powering electronic watch). *Source:* Reproduced with permission [98]. © 2014, Elsevier Publishing.

maximum power density of 6.8 kW kg^{-1} . Moreover, the as-fabricated device exhibited superior cyclic stability even when bent or twisted.

Unfortunately, most carbon-based anodes are relatively low in capacitance due to the electrochemical double layer energy storage mechanism. To this end, effective strategies of achieving high-energy-dense AFSCs has been extensively developed by employing pseudocapacitive anodes such as functionalized carbon, transition metal oxides, transition metal nitrides, conductive polymers, etc. [90] Recently, Wang et al. [90] creatively applied electrochemical activation to CC (Figure 1.4a), which were rarely employed as SC electrode materials because of its intrinsic low capacitance as a result of the small surface area and poor electrochemical activity [32]. The obtained electrochemically activated carbon cloth (EACC) anode was coupled with $\text{MnO}_2@ \text{TiN}$ loaded on CC as cathode to fabricate a novel sandwich-type AFSC (denoted as $\text{MnO}_2@ \text{TiN} // \text{EACC}$) with an extended operation voltage window of 2V (Figure 1.4b). Besides the broadened voltage window, the impressively boosted capacitance of EACC due to the roughened surface and the introduction of oxygen-containing groups on the surface for redox reactions also contribute to an excellent energy density as high as 1.5 mWh cm^{-3} , which enables its successful application in powering light emitting diode (LED) indicator even under bent condition (Figure 1.4c).

1.3.1.2 Transition Metal Oxide Anodes

Transition metal oxides can generate reversible redox reactions on the surface or even in the bulk during charging/discharging, which results in much higher capacitances compared to carbon-based anodes. By integrating transition metal oxides with flexible current collectors as as

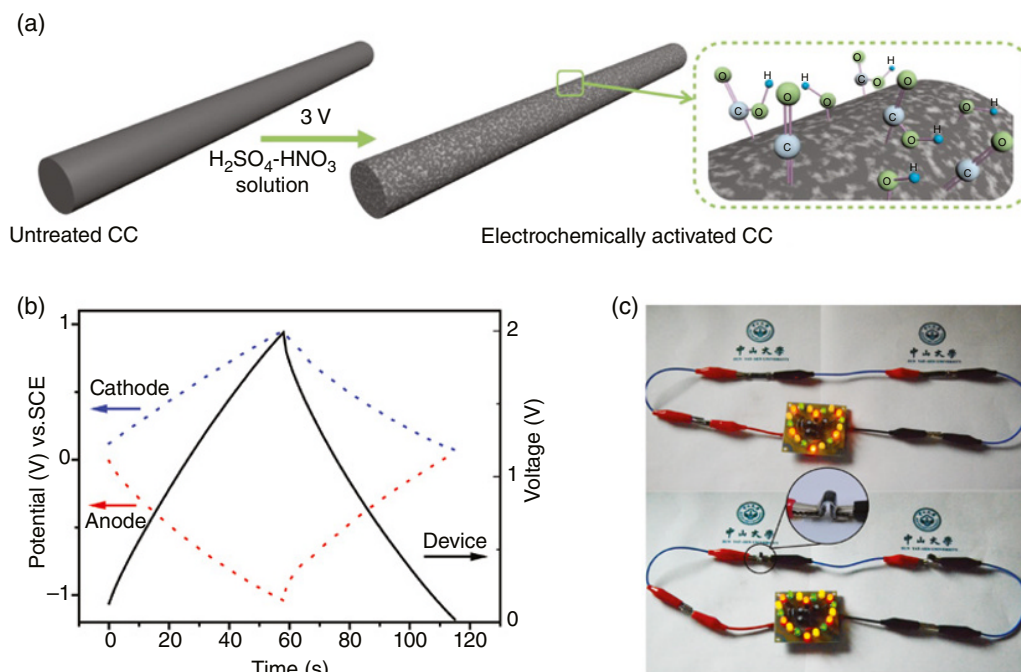


Figure 1.4 (a) Schematic diagram of the CC activation process. (b) Galvanostatic charge/discharge curve and potential distribution curve for the $\text{MnO}_2@ \text{TiN} // \text{EACC}$ device at 6 mA cm^{-2} . (c) A LED indicator powered by the tandem straight and bended $\text{MnO}_2@ \text{TiN} // \text{EACC}$ devices. *Source:* Reproduced with permission [90]. © 2015, Wiley-VCH.

pseudocapacitive anodes, the energy density of AFSC can be drastically enhanced. For example, Yang et al. [54] grew α - MnO_2 nanowires (NWs) and amorphous Fe_2O_3 nanotubes (NTs) on flexible carbon textile as the pseudocapacitive cathode and anode respectively (Figure 1.5a) to fabricate a sandwich-type flexible asymmetric pseudocapacitor (Figure 1.5b). The as-fabricated sandwich-type AFSC operates at a maximum cell voltage of 1.6 V (Figure 1.5c) and delivers high energy density of 0.55 mWh cm^{-3} (Figure 1.5d). Two devices connected in series can readily operate a blue LED after charging (Figure 1.5d inset), indicating the potential of the AFSC in future applications. Similarly, a novel flexible all-solid-state asymmetric SC fabricated with a carbon-fabric-loaded $\text{WO}_{3-x}/\text{MoO}_{3-x}$ core/shell nanowires anode and a polyaniline cathode was reported by Xiao and his co-workers. The device showed satisfactory energy density (1.9 mWh cm^{-3}), impressive cyclic stability, as well as good mechanical flexibility.

1.3.1.3 Transition Metal Nitride Anodes

Owing to the high conductivity and transition metal sites with multiple valence states, transition metal nitrides are emerging as promising pseudocapacitive anode materials with fast and reversible redox reactions. Many transition metal nitrides have been exploited for AFSCs, such as

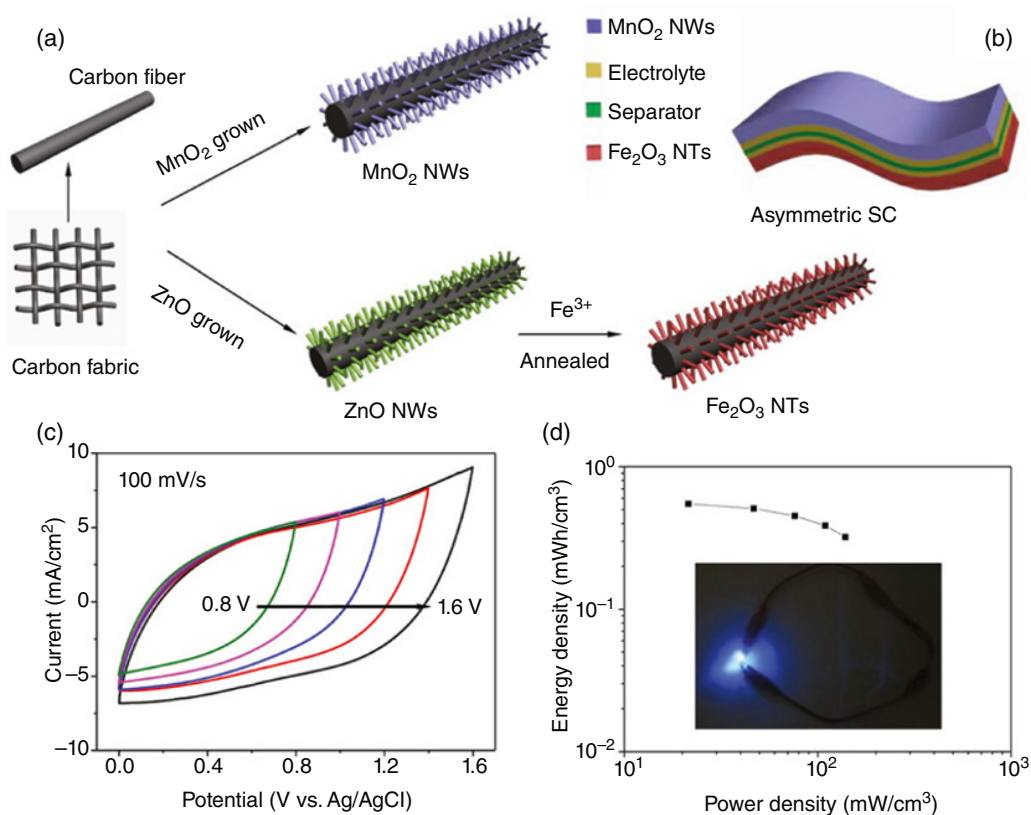


Figure 1.5 (a) Schematic diagram illustrating the synthesis procedure of MnO_2 NWs and Fe_2O_3 NTs on carbon cloth. (b) Schematic sketch illustrating the designed asymmetric supercapacitor device. (c) CV curves of the assembled solid-state AFSC device collected in different scan voltage windows. (d) Ragone plots of the solid-state AFSC device. Inset shows a blue LED powered by the tandem AFSC devices. *Source:* Reproduced with permission [54]. © 2014, American Chemical Society.

titanium nitride, vanadium nitride, tungsten oxynitride, iron nitride, etc., with high performances comparable to transition metal oxide anodes [91, 99–101]. For instance, Fan's group successfully fabricated an all-metal nitrides solid-state asymmetric SC, where the titanium nitride (TiN) cathode and iron nitride (Fe_2N) anode were grown on CC-loaded graphene nanosheets (GNS) using atomic layered deposition followed by calcination under ammonia atmosphere (Figure 1.6a).

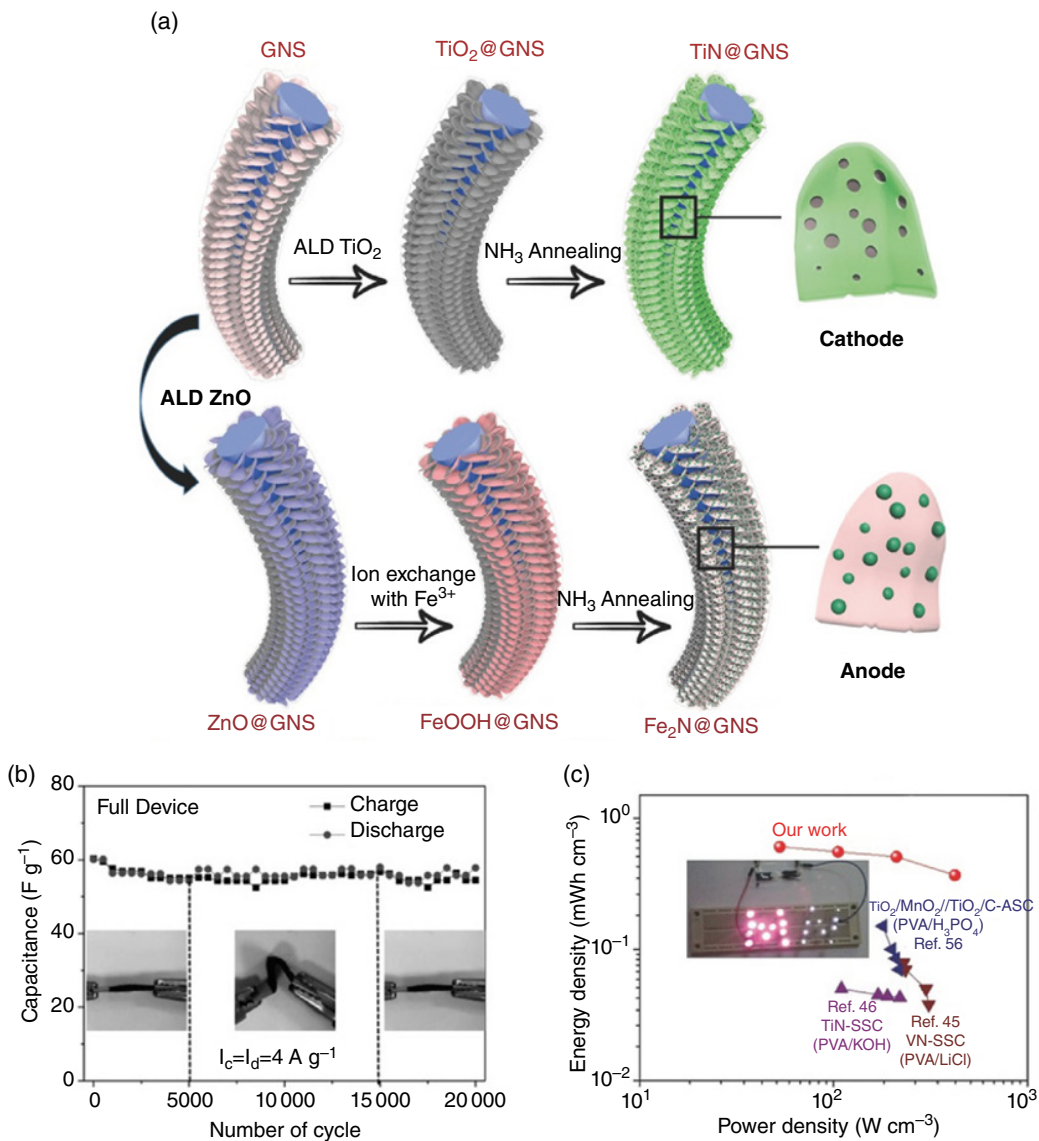


Figure 1.6 (a) Schematics of the fabrication processes of metal nitride cathode and anode materials. (b) Cycling performance of full device at 4 A g^{-1} in 20 000 cycles with different bending situations. (c) Ragone plots of quasi-solid-state TiN- Fe_2N AFSC in comparison with other PVA-based solid electrolyte SFSCs and AFSCs. Inset: pink and white LEDs in parallel are lit up by two full devices in tandem. Source: Reproduced with permission [101]. © 2015, Wiley-VCH.

The porous configuration of TiN and homogeneous distribution of Fe₂N nanoparticles contribute to the extraordinary cycling durability ($\approx 98\%$ capacity retention after 20000 cycles) of the fabricated quasi-solid-state AFSC device using PVA/LiCl polymer gel as neutral electrolyte (Figure 1.6b). The AFSC device achieved a maximum energy density of 0.61 mWh cm^{-3} and a maximum power density of 422.7 mW cm^{-3} , which were substantially higher than those of transition-metal-nitride-based SCs and PVA-based solid-state SCs (Figure 1.6c). Lu's group has reported various AFSCs using CC-loaded transition metal nitride anodes in recent years. For example, they used neutral PVA/LiCl polymer gel electrolyte to effectively stabilize porous VN NWs anode, and paired it with VO_x NWs cathode to assemble a stable and high-performance quasi-solid-state AFSC device with a high output voltage of 1.8 V [91]. Furthermore, the VO_x/VN-AFSC device was able to deliver an impressive volumetric capacitance of 1.35 F cm^{-3} , a highest energy density of 0.61 mWh cm^{-3} and extraordinary cycling stability with 12.5% loss of capacitance after 10000 cycles. They also prepared holey tungsten oxynitride (WON) nanowires on CC through the annealing of WO₃ precursor nanowires in ammonia atmosphere [100]. The as-fabricated AFSC device with WON NWs anode and MnO₂ cathode could deliver a high working voltage of 1.8 V and volumetric capacitance of 2.73 F cm^{-3} . The maximum energy density of MnO₂/WON AFSC device was 1.27 mWh cm^{-3} at a power density of 0.62 W cm^{-3} , which has transcended many reported AFSC devices.

1.3.1.4 Conductive Polymer Anodes

Conductive polymers are promising candidates as pseudocapacitive materials owing to their good conductivity and reversible redox reactions during charging/discharging, but they are mostly applied as cathode materials while rarely studied as anode materials for AFSCs. Recently, Wang et al. synthesized 150 WO₃@PPy nanowires on carbon fibers as the anode and grew Co(OH)₂ nanowires on carbon fabric as the cathode for AFSC device. The as-fabricated AFSC device exhibited apparent pseudocapacitive behavior within a stable potential range of 0–1.6 V. The maximum volumetric capacitance of 2.8 F cm^{-3} was achieved at a scan rate of 20 mV s^{-1} . Moreover, the asymmetric supercapacitor (ASC) device delivered an energy density as high as 1.03 mWh cm^{-3} .

1.3.2 Fiber-Type ASCs

Despite distinct advances, the planar-shaped SCs are still insufficient in deformability for weaving into textiles or integrating into linear-shaped electronics. In this regard, researchers have creatively assembled electrodes with one-dimensional geometry to fabricate fiber-type AFSCs. Fiber-shaped AFSCs have been developed into multiple configurations including parallel type, wrap type, coaxial-helix type and two-ply yarn type, in order to effectively meet the demands of different wearable energy textiles, including sensing [102–104], communication [105], and storage [106].

1.3.2.1 Parallel-Type Fiber AFSCs

For a parallel-type fiber AFSC, two fiber-shaped electrodes are assembled side-by-side, separated by gel/polymer electrolyte, and finally supported on a flat substrate [60, 107–109]. For instance, Yu et al. [109] reported a parallel type all-solid-state asymmetric micro-SC using MnO₂-deposited rGO/SWCNT fiber as the cathode (denoted as GCF/MnO₂-10) and an N-doped rGO/SWCNT fiber as the anode (denoted as GCF/N₂) (Figure 1.7a). By fully utilizing the potential window of both cathode (0~0.9 V) and anode (−0.9~0 V), the device showed a high output voltage of 1.8 V (Figure 1.7b). Excellent electrochemical performances such as good cycling stability

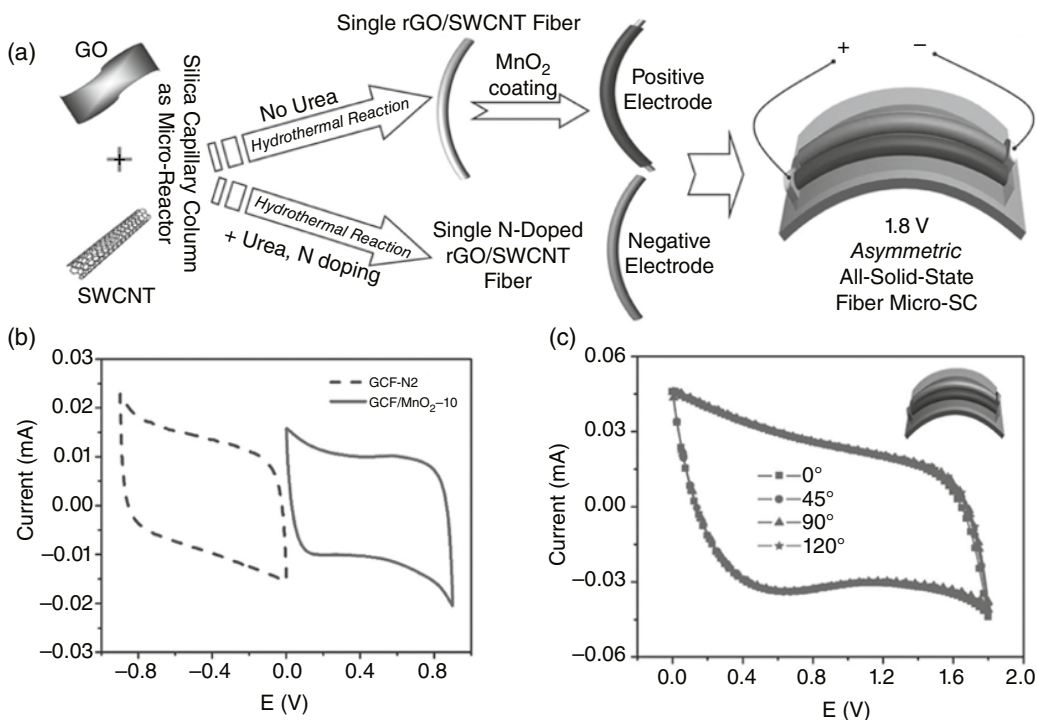


Figure 1.7 (a) Schematic illustration of the design and fabrication of the asymmetric fiber-based micro-SC. (b) Comparative CV curves obtained for the GCF-N2 and GCF/MnO₂-10 fibers at the scan rate of 10 mV s⁻¹. (c) CV curves of one asymmetric micro-SC, which are bended at different angles. *Source:* Reproduced with permission [109]. © 2014, Wiley-VCH.

(87% capacitance retention after 10 000 cycles), high energy density (5 mW h cm⁻³) and power density (929 mW cm⁻³) were also achieved. Furthermore, such device geometry exhibited promising mechanic stability under different bending states (Figure 1.7c). This asymmetric micro-SC device was testified as a reliable power source for a ZnO film-based UV photodetector, suggesting its promising potential in future applications.

1.3.2.2 Wrap-Type Fiber AFSCs

The design of a wrap-type AFSC is very similar to that of a parallel-type fiber AFSC, which encapsulates two electrodes into a protective flexible tube instead of placing them on a flexible substrate [53, 59, 62, 110–112]. Recently, Lu and his co-workers [112] successfully synthesized N and low valence-state Mo dual-doped MoO₃ nanowires on carbon fibers, which was coupled with MnO₂@TiN-loaded carbon fiber cathode and sealed with heat-shrinkable tube to fabricate a wrap type solid-state ASC (denoted as MnO₂@TiN//N-MoO_{3-x}) (Figure 1.8a). The galvanostatic charge/discharge (GCD) curves of MnO₂@TiN//N-MoO_{3-x} with different current densities in Figure 1.8b indicate that the stable operating voltage of the device reaches a significantly high value of 2.0V. The ASC device also shows superior rate capability when current density increased by 15 folds (Figure 1.8c). More importantly, the excellent flexibility and mechanic robustness enabled the fiber AFSC device to perfectly maintain its electrochemical performances in bent and even knotted conditions (Figure 1.8d). Benefiting from the ultrahigh output voltage and Faradaic

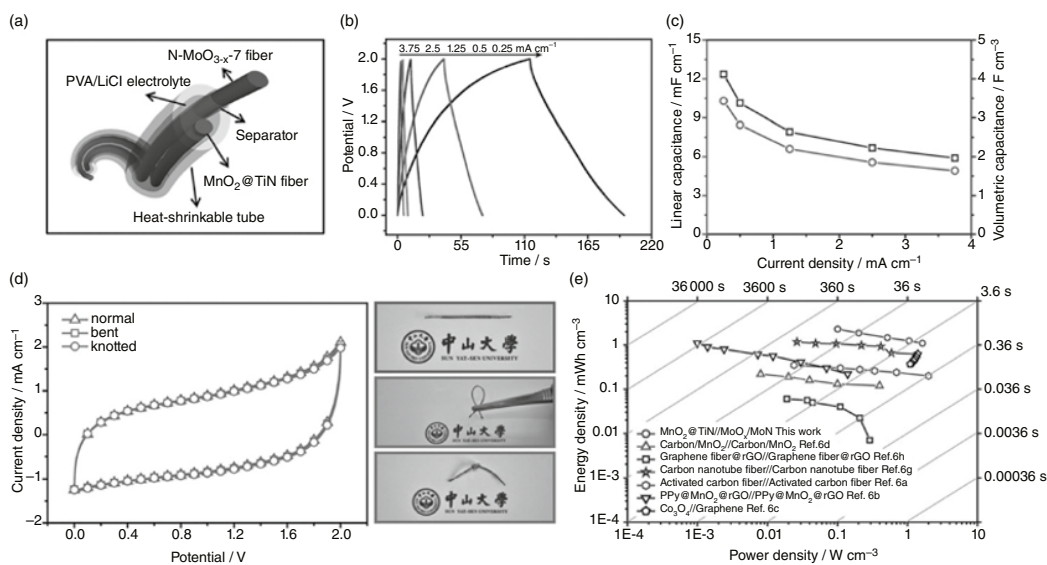


Figure 1.8 (a) Schematic illustration of the as-assembled fiber-shaped MnO₂@TiN/N-MoO_{3-x}-ASC device. (b) GCD curves of our fiber-shaped AFSC device. (c) Linear capacitances and volumetric capacitances of the fiber-shaped AFSC device as a function of current density. (d) CV curves collected at 100 mV s⁻¹ for the fiber-shaped AFSC device under different conditions (left) and corresponding device pictures (right). (e) Ragone plots for the fiber-shaped AFSC device and other recently reported fiber-shaped FSCs. Source: Reproduced with permission [112]. © 2016, Wiley-VCH.

electrodes with improved conductivity, the $\text{MnO}_2@\text{TiN}/\text{N-MoO}_{3-x}$ device exhibited a maximum energy and power density of 2.29 mWh cm^{-3} and 1.64 W cm^{-3} respectively, outperforming many other fiber-shaped SC devices reported (Figure 1.8e).

1.3.2.3 Coaxial-Helix-Type Fiber AFSCs

By helically wrapping a wire shape axial electrode with another wire electrode, coaxial-helix-type ASCs with core-shell cable-like structures have been creatively explored [86, 113–117]. For example, the Thomas group [117] fabricated a novel cable-like coaxial-helix-type AFSC as illustrated in

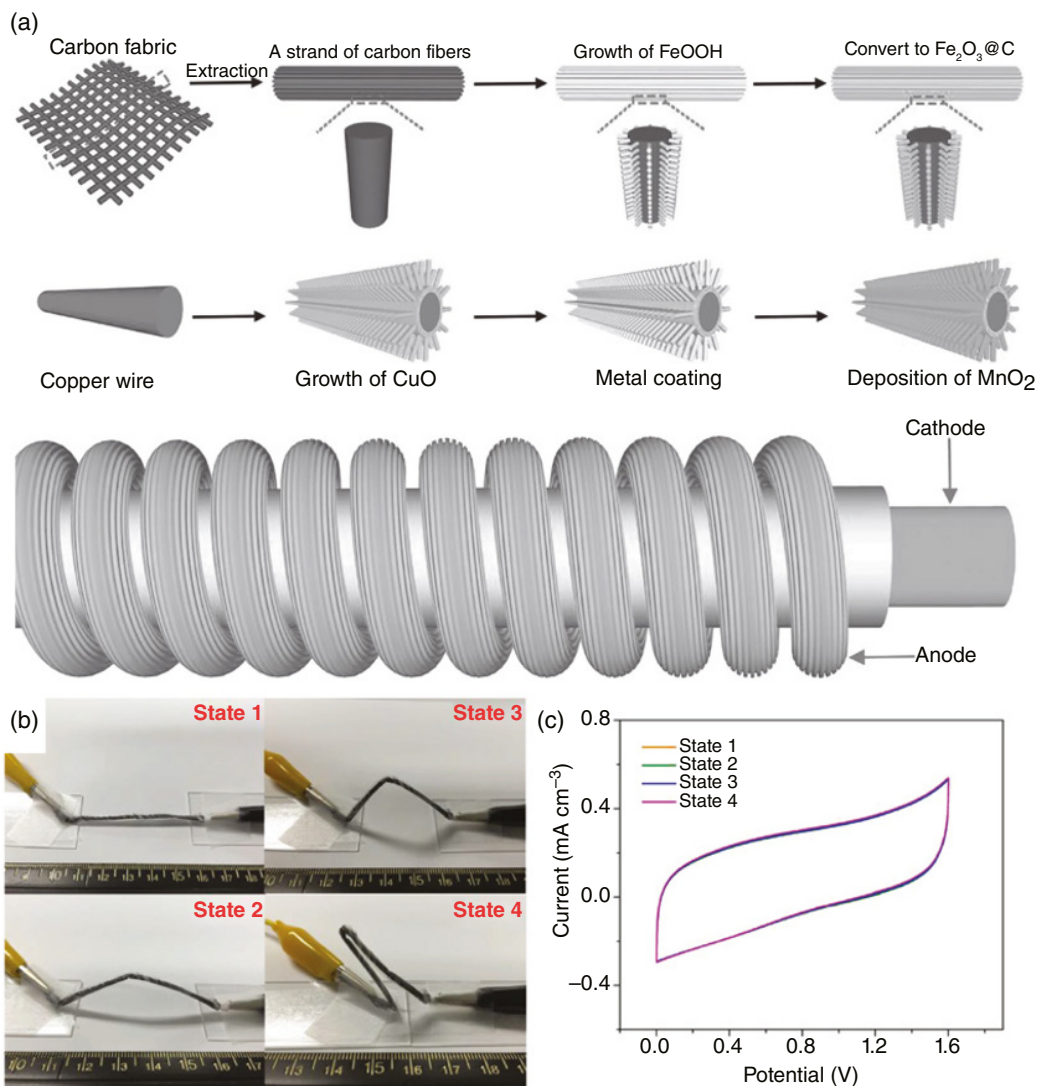


Figure 1.9 (a) Schematics illustration shows the fabrication process of an anode and a cathode, respectively, and the structure of a coil-type asymmetric supercapacitor electrical cable. (b) Optical images of a coil-type asymmetric supercapacitor electrical cable at different bending states. (c) CV curves obtained at different bending states at 200 mVs^{-1} . Source: Reproduced with permission [117]. © 2015, Wiley-VCH.